NIH Public Access
Author Manuscript
Dev Dyn. Author manuscript; available in PMC 2010 September 1.

Published in final edited form as:
Dev Dyn. 2009 September ; 238(9): 2211–2222. doi:10.1002/dvdy.21956.

Different Roles For KIF17 and Kinesin II In Photoreceptor Development and Maintenance

Christine Insinna[1], **Monica Humby**[1], **Tina Sedmak**[2], **Uwe Wolfrum**[2], and **Joseph C. Besharse**[*,1]

[1]Department of Cell Biology, Neurobiology and Anatomy, Medical College of Wisconsin, 8701 Watertown Plank Rd, Milwaukee, WI 53226, USA

[2]Johannes Gutenberg University of Mainz, Institute of Zoology, Cell and Matrix Biology, Muellerweg 6, D-55099 Mainz, Germany

Abstract

Kinesin 2 family members are involved in transport along ciliary microtubules. In *C. elegans* channel cilia, kinesin II and OSM-3 cooperate along microtubule doublets of the axoneme middle segment whereas OSM-3 alone works on microtubule singlets to elongate the distal segment. Among sensory cilia, vertebrate photoreceptors share a similar axonemal structure with *C. elegans* channel cilia, and deficiency in either kinesin II or KIF17, the homologue of OSM-3, results in disruption of photoreceptor organization. However, direct comparison of the two effects is confounded by the use of different species and knockdown strategies in prior studies. Here, we directly compare the effects of dominant negative kinesin II and KIF17 expression in zebrafish cone photoreceptors. Our data indicate that dominant negative kinesin II disrupts function at the level of the inner segment and synaptic terminal and results in cell death. In contrast, dominant negative KIF17 has no obvious effect on inner segment or synaptic organization but has an immediate impact on outer segment assembly.

Keywords

KIF17; kinesin II; photoreceptors; ciliogenesis; IFT

Introduction

Numerous studies have demonstrated that heterotrimeric members of the kinesin 2 family, referred to here as kinesin II, are required for intraflagellar transport (IFT) and ciliogenesis (Kozminski et al., 1995; Morris and Scholey, 1997; Cole et al., 1998; Nonaka et al., 1998). Although kinesin II clearly plays a role as an anterograde IFT motor in *Chlamydomonas rheinhartii* and *Caenorhabditis elegans*, the involvement of at least one additional ciliary kinesin in *C.elegans* has led to a more complex view of kinesin's role in ciliogenesis. Some studies suggest that kinesin II might play a role in loading cargo on IFT proteins at the base of the cilium as well as transporting them along the axoneme (Scholey, 2008). Furthermore, mutations in two of the subunits (KAP-1, KLP-11) of *C.elegans* kinesin II have no immediate effect on ciliary axoneme formation in sensory cilia (Snow et al., 2004; Evans et al., 2006). This observation may be explained by the finding that another kinesin 2 family member,

*Correspondence: Dr. Joseph C. Besharse, Department of Cell Biology, Neurobiology and Anatomy, Medical College of Wisconsin, 8701 Watertown Plank Rd, Milwaukee, WI 53226, Telephone: (414) 456-8260, Fax: (414) 456-6517, Email: jbeshars@mcw.edu.

NIH-PA Author Manuscript
NIH-PA Author Manuscript
NIH-PA Author Manuscript

NIH-PA Author Manuscript

NIH-PA Author Manuscript

NIH-PA Author Manuscript

OSM-3, compensates for kinesin II loss of function. On the other hand, loss of OSM-3 function leads to failure of distal axoneme elongation (Snow et al., 2004; Evans et al., 2006).

Recent work implicates both kinesin II and KIF17, the vertebrate homologue of OSM-3, in assembly of the photoreceptor outer segment (OS), a modified sensory cilium (Horst et al., 1990). For example, the conditional and photoreceptor specific knockout in mice of a kinesin II subunit, KIF3A, causes an ectopic accumulation of opsin in the IS that leads to photoreceptor degeneration (Marszalek et al., 2000; Jimeno et al., 2006) while a dominant negative form of the KIF3B subunit expressed during early development in *Xenopus* rods causes disrupted photoreceptor organization and cell death (Lin-Jones et al., 2003). In contrast, knock-down of KIF17 in zebrafish photoreceptors disrupts or ablates OS formation with little initial effect on the other segments of the cell (Insinna et al., 2008). Although these studies implicate both kinesin 2 family members in OS formation, direct comparison of their relative roles in photoreceptors is not possible because of the use of different strategies in different species.

In order to directly compare the relative roles of these two kinesin 2 family members in photoreceptors using similar approaches in the same species, we first produced KIF3B morphants for comparison to our previous study of KIF17 morphants (Insinna et al., 2008). This approach was generally unsuccessful because of early developmental anomalies that prevented formation of a photoreceptor layer. We, therefore, used a late onset, cone specific promoter (Kennedy et al., 2007) to drive expression of two previously described dominant negative constructs (Lin-Jones et al., 2003; Chu et al., 2006) of KIF3B (DNKIF3B) and KIF17 (DNKIF17) during development of zebrafish cones. Consistent with a previous report, DNKIF3B over-expression resulted in photoreceptor death (Lin-Jones et al., 2003). However, initial signs of disruption with DNKIF3B were within membrane systems of the IS and in the formation of synaptic ribbons at the synaptic terminal. In contrast, over-expression of DNKIF17 led to immediate OS maintenance defects involving disruption of OS discs. This suggests that while the two motors have overlapping roles in photoreceptor IFT, kinesin II also performs independent functions in photoreceptors distinct from its role in IFT.

Results

Kinesin II co-localizes and associates with KIF17 in both mice and zebrafish

Prior immunofluorescence studies established that KIF17, KIF3A and KIF3B are localized in the synaptic terminal, the inner segment (IS) and along the axoneme of vertebrate photoreceptors (Beech et al., 1996; Muresan et al., 1997; Muresan et al., 1999; Whitehead et al., 1999; Insinna et al., 2008). Additionally, the distribution of kinesin superfamily proteins (KIFs) was characterized by immuno-electron microscopy in sunfish photoreceptors using anti-LAGSE, an antibody that recognizes the conserved motor domain of KIFs (Beech et al., 1996). We focused our ultrastructural analysis on the localization of the kinesin II subunit, KAP3, and KIF17 in mouse photoreceptors using a pre-embedding electron microscopy (EM) approach (Maerker et al., 2008). Thick sections of fixed mouse retinae were cracked and subsequently incubated with polyclonal or monoclonal antibodies for KIF17 or KAP3 followed by silver enhancement and osmium fixation before final embedment in resin. As expected, labeling with both antibodies was detected along microtubules of the entire axoneme in the OS (Fig. 1A-B,D-E). Labeling was stronger at the base but was still detected in the most distal part of the OS. Interestingly, we were unable to detect signal with either antibody in longitudinal sections of the connecting cilium (CC) (Fig. 1A and E). This observation is consistent with previous studies of longitudinal sections labeled with the LAGSE antibody (Beech et al., 1996). However, cross-sections of the CC revealed strong labeling for KAP3 (Fig. 1B) and KIF17 (Fig. 1D), showing that the lack of staining in longitudinal sections is likely due to a barrier to access of antibodies (Maerker et al., 2008). Our results show that KIF17 and kinesin II co-localize in structures that are critical for the inter-segmental transport of material through

NIH-PA Author Manuscript

NIH-PA Author Manuscript

NIH-PA Author Manuscript

the photoreceptor CC. KAP3 and KIF17 were also found at the periciliary region of the IS and in the vicinity of the basal body (Fig. 1A and E), and in the collar-like extension of the IS adjacent to the CC (Fig. 1E asterisks). Furthermore, KAP3 was localized along ER and Golgi membranes as well as tubulo-vesicular elements within the IS (Fig.1C).

Kinesin II is known to exist in a complex with IFT proteins isolated by immunoprecipitation (Cole et al., 1998; Baker et al., 2003; Qin et al., 2004), and we have recently demonstrated that KIF17 is associated with IFT complexes as well (Insinna et al., 2008). This implies the existence of IFT complexes associated with both motors. We, therefore, evaluated the possible co-immunoprecipitation (IP) of KIF17 and the three kinesin II subunits from mouse retinal extract (Fig. 1F). Immunoprecipitates were immunoblotted for the three individual subunits of kinesin II (Fig. 1F, left) as well as IFT88 and KIF17 (Fig. 1F, right). KIF3B and KIF3A were found to migrate at ~ 95 kDa and ~ 85 kDa respectively. The KIF17 antibody co-precipitated a subpopulation of kinesin II and, reciprocally, the kinesin II antibody co-precipitated a population of KIF17. The weak intensity of the Western blot for KIF3A in the KIF17 IP compared to the kin II IP (Fig. 1F) was consistent in our experiments. This may be explained by the previous observation that KIF3A exists independent of KIF3B in a complex with synaptic ribbons in photoreceptors (Muresan et al., 1999). Since the kin II IP antibody recognizes both KIF3A and KIF3B, it would likely bring down both ribbon bound KIF3A as well as KIF3A in the heterotrimeric complex. While both the KIF17 and kinesin II antibodies immunoprecipitated roughly equal amounts of IFT88, the relative abundance of KIF3B and KIF17 in the two IPs was different. This suggests that multiple IFT complexes containing either KIF17 or kinesin II are likely to be present in mouse retinae; it is also likely that some complexes contain both motors.

A similar IP was conducted using zebrafish retina (Fig. 1G). However, the individual mouse kinesin II subunit antibodies did not cross-react with the zebrafish proteins. Therefore, we used the general kinesin II antibody, K2.4 (Cole et al., 1993), that recognizes both KIF3A and KIF3B in the western blotting. In the kinesin II IP, two bands at ~ 80/90 KDa correspond to KIF3A and KIF3B (Fig. 1G). The antibody to KIF17 co-precipitated a small but consistent amount of kinesin II from zebrafish retinae (Fig. 1G). Interestingly, in zebrafish tissue, the anti-KIF17 antibody pulled down mainly KIF3A and a smaller amount of KIF3B. However, this could reflect differences in affinity of the K2.4 antibody for the two subunits in western blots rather than kinesin complexes deficient in KIF3B. Our previous work in zebrafish indicates that the complex immunoprecipitated with the KIF17 antibody also includes IFT proteins (Insinna et al., 2008).

Knock-down of the KIF3B Causes Early Embryonic Defects

In order to knock-down KIF3B expression in developing zebrafish embryos for direct comparison to our prior work on KIF17 knockdown (Insinna et al., 2008), we designed three antisense morpholino oligonucleotides: a translation-blocking morpholino (AKIF3B), a morpholino directed at the exon 2 splice donor site (SpKif3B) and a control morpholino containing the sense sequence of *kif3b* mRNA. The majority of morphants (~ 85 %) injected at the one cell stage with a high dose (500 μM) of translation-blocking or splice-blocking morpholino died at 24h post fertilization whereas controls were normal. Lowering the dose to 250 μM improved the survival rate for both morpholinos to about 50%. The translation-blocking morpholino caused a dose-dependent decrease in KIF3B expression (Fig. 2B). The depletion of KIF3B also reduced KIF3A, but KIF17 expression was not affected by the depletion of kinesin II (Fig. 2B). A similar depletion of KIF3B was seen in morphants injected with the splice-blocking morpholino (Fig. 2C), but the parallel reduction in KIF3A was not as dramatic.

NIH-PA Author Manuscript

NIH-PA Author Manuscript

NIH-PA Author Manuscript

Although most KIF3B morphants died, those that survived through 3 dpf had multiple abnormalities including heart edema, small eyes, hydrocephalus and strong body curvature (Fig. 2A, AKIF3B 500 μM). Semi-thin sections of their retinae showed a strong developmental delay phenotype compared to controls with defects in lamination and optic stalk formation and a lack of photoreceptor differentiation (Fig. 2E). The absence of photoreceptors with OS precluded analysis of OS formation in these embryos. We, therefore, studied photoreceptors in embryos injected with either AKIF3B or SpKIF3B at 250 μM (Fig. 2D). Although a greater number of embryos survived with less severe developmental anomalies, light microscopy (Fig. 2D) and ultrastructural analysis (Fig. 2D insets) of their retinae showed that OS formation was indistinguishable from controls. This result, however, does not necessarily imply a lack of a requirement of kinesin II because at low morpholino concentration sufficient kinesin II may have been present in photoreceptors.

Our results with antisense morpholinos are consistent with conventional gene knockouts in mice for both KIF3B and KIF3A, which showed a requirement in early development prior to retinal differentiation and photoreceptor formation (Marszalek et al., 1999; Nonaka, et al., 1998). Although toxic effects of the morpholinos cannot be ruled out, the similar effects of both a splice blocking and translation blocking morholino suggests that the effects were specific. Furthermore, none of these early developmental defects were observed in KIF17 morphants (Insinna et al., 2008). Nonetheless, with the delay in retinal development and lack of photoreceptors in KIF3B morphants direct comparison of the effects of morpholino knockdown of the two motors on photoreceptor OS formation was not possible.

DNKIF3B in zebrafish cones causes acute IS and synaptic defects

As an alternative strategy for comparison of the roles of kinesin II and KIF17 in OS maintenance, we directed the expression of dominant negative KIF3B (DNKIF3B) and dominant negative KIF17 (DNKIF17) to cone photoreceptors using a cone transducin alpha (Ta-CP) promoter, which is known to induce transgene expression in greater than 50% of the cones at 3-5 dpf (Kennedy et al., 2007). The DNKIF3B and DNKIF17 constructs were designed so that the motor domain of each protein was replaced by GFP (Le Bot et al., 1998; Lin-Jones et al., 2003; Chu et al., 2006). Although dimerization behavior, which depends on the coil-coiled stalk is maintained, these proteins are non functional. Prior work using this DNKIF3B construct showed that the non-functional KIF3B protein is still able to associate with endogenous kinesin II subunits, which results in the inactivation of the whole complex (Le Bot et al., 1998).

We injected embryos with the DNKIF3B or DNKIF17 constructs at the one cell stage, screened for GFP fluorescence in the eye at 3 dpf and examined retinae by light microscopy and EM at 5 dpf. Consistent with prior work (Kennedy et al., 2007), fluorescence from GFP alone (control) at 5 dpf was detected throughout the eye with areas representing 15-40 % of the cones expressing GFP at high levels (Fig. 3A); a similar distribution pattern for both of the GFP tagged dominant negative proteins was observed (Fig. 3B and C). At this stage, retinae are composed of ~ 90 % cones with outer segments approximately half of their adult length; cone outer segments are shorter and less developed at the retinal periphery. Our results (Fig. 3) suggest that the Ta-CP promoter drives protein expression efficiently in the great majority of cones. Rods constitute only about 10% of the total number of photoreceptors and are present mainly at the ventral periphery (Branchek and Bremiller, 1984; Kljavin, 1987).

Since cones in the central retina are older and are at more advanced stage OS formation than those at the periphery at the time of onset of transgene expression, the dominant negative phenotypes are considered separately for the central and peripheral retina (Fig. 4 and 5). In embryos injected with DNKIF3B we found that 15-30% of the cones were in an apoptotic state as evidenced by both nuclear and cytoplasmic compaction. These dead or dying cones were

NIH-PA Author Manuscript

NIH-PA Author Manuscript

NIH-PA Author Manuscript

seen at the retinal center and to a lesser extent at the ventral periphery, which contains the most recently developed cones (Fig. 4A and D, Fig. 5B). In contrast, control retinae from embryos injected with the Ta-CP promoter construct driving GFP were devoid of apoptotic cells (data not shown). This suggests that the degeneration and death of developing cones is the result of accumulation of the dominant negative protein.

Ultrastructural defects due to DNKIF3B expression, largely restricted to the inner segment (IS), ranged from mild to severe. Mild IS defects generally involved enlargement of the cytoplasmic domain in the mitochondria rich ellipsoid region (Fig. 6B-D). This was mainly seen at the retinal periphery in cells that maintained normal structure and length of the OS (Fig. 5B, Fig. 6B-D). In more severe cases nuclear and inner segment compaction was seen in cells with normal organization of OS discs (Fig. 6E-F). Finally, accumulation of large vesicles at in the ellipsoid region of the inner segment accompanied by enlargement of the apical IS region was seen in ~ 10% of the cones (Fig. 5B, Fig. 6G-I). In contrast, controls had a tightly compacted IS at the level of the ellipsoid and large vacuoles and compacted cells were not seen (Fig. 5A, Fig. 6A). In general, OS maintained a relatively well-organized structure with normal disc stacking in cones showing severe disorganization of the inner segment.

To determine if cone opsin was mislocalized in cells expressing DNKIF3B protein cryostat sections were labeled with anti-cone opsin antibodies and examined for both GFP and opsin fluorescence. In retinae of embryos injected with the Ta-CP/GFP construct, opsin was highly expressed in the cone OS but was not detectible in the inner segment or cone terminals in the outer plexiform layer (Fig. 3A). In contrast, in retinae expressing DNKIF3B cone opsin was mislocalized and was abundant in cone terminals in the outer plexiform layer across the entire retina (Fig. 3B).

To complete our ultrastructural analysis we also examined cone synaptic pedicles in control compared to DNKIF17 and DNKIF3B expressing embryos (Fig. 7). Both control (Fig. 7A-C) and DNKIF17 (Fig. 7D-F) expressing embryos had well developed cone pedicles with post-synaptic invaginations and synaptic ribbons associated with presynaptic membranes (Fig. 7 C and F, insets). However, synaptic ribbons were rarely seen in pedicles of DNKIF3B expressing embryos (Fig. 7G-I). Instead, pedicles with post-synaptic invaginations (Fig 7I, inset), but lacking ribbons were seen throughout the retina. In the rare instances when ribbons were detected, they were not associated with the pre-synaptic membrane (Figure 7I). These findings suggest that KIF3B plays an additional role in synaptic morphogenesis, consistent with prior work showing that it functions in axonal transport in addition to IFT (Muresan, 2000).

DNKIF17 in zebrafish cones disrupts OS elongation and early disc morphogenesis

In contrast to our results with DNKIF3B, EM analysis of cone photoreceptors expressing DNKIF17 (Chu et al., 2006) at 5 dpf revealed little if any evidence of cell death in the photoreceptor layer. However, the late developing cones at the periphery failed to elongate their OS compared to control embryos (Figs. 4E, 5C, 8A-D). Furthermore, in developing cells with short OS, disc edges on the opposite side from the CC were abnormal and vesicle-like structures accumulated in the OS (Fig. 8A-C). This phenotype was also observed to a lesser extent in OS localized at the central retina. In the retinal center the OS of DNKIF17-expressing retinae were normal in length but many accumulated membrane vesicles, particularly at the OS base (Fig. 8E). This area of the OS is known as the disc-forming region, and our results suggest that KIF17 is involved in the transport of elements essential for disc morphogenesis. In our analysis of DNKIF3B and DNKIF17 the rod photoreceptors, which did not express the dominant negative protein, had normal structure (Fig. 8F).

In contrast to cones expressing the DNKIF3B construct (Fig. 3B), little if any cone opsin mislocalization was detected in cells expressing DNKIF17 (Fig. 3C). This suggests that despite

NIH-PA Author Manuscript

NIH-PA Author Manuscript

NIH-PA Author Manuscript

anomalous disc morphogenesis within the OS cone opsin is still delivered to the OS segment normally. Finally, as mentioned above the development of cone synaptic terminals was normal (Fig. 7D-F) in photoreceptors exhibiting disrupted OS formation.

Discussion

Our immuno-EM analysis of the anti-KAP3 and anti-KIF17 labeling in mouse photoreceptors confirm previous studies conducted in fish photoreceptors using anti-KIF3A and anti-KIF17 antibodies (Beech et al., 1996; Insinna et al., 2008). Indeed, both kinesin II and KIF17 are associated with microtubule doublets of the CC and axonemal microtubules that extend distally into the OS. In addition, both kinesins were found in the periciliary compartment of the IS, the basal body region and the collar-like IS extension, which is thought to be the pathway for the inter-segmental transport and the site for IFT complex assembly (Tam et al., 2000; Deane et al., 2001; Maerker et al., 2008). Furthermore, our IP data suggest the existence of protein complexes containing the two kinesins and IFT proteins in both mouse and zebrafish photoreceptors (Baker et al., 2003; Insinna et al., 2008). Additionally, our finding that anti-KIF17 and kinesin II antibodies co-precipitated similar amounts of IFT88, but differentially co-precipitated kinesin II or KIF17 suggests the existence of IFT complexes containing either KIF17 or kinesin II. Indirect evidence for such complexes has been found in *C.elegans* AWB cilia where the KIF17 homologue, OSM-3, has been suggested to be associated with an IFT complex independent of kinesin II (Mukhopadhyay et al., 2007).

Combined, our localization and IP data are consistent with both cooperative and independent functions of the two kinesins within the OS. In *C.elegans* channel cilia it has been proposed that kinesin II and OSM-3 behave cooperatively to build the middle (proximal) segment of the axoneme, but that OSM-3 alone is required for the distal segment extension (Snow et al., 2004; Evans et al., 2006; Pan et al., 2006). Although a similar dichotomy of function is possible along the axoneme of zebrafish photoreceptors, the situation is more complicated because both KIF17 morphants and those expressing DNKIF17 exhibit severe OS ablation or a strong proximal OS defect that is not seen in DNKIF3B expressing cells. This suggests that in photoreceptors KIF17 plays a non-redundant role in proximal OS assembly, possibly by transporting cargo essential for this process.

An important finding in this analysis is cone opsin mislocalization in cells expressing DNKIF3B, but not in those expressing DNKIF17 (see Fig. 3). The fact that opsin localizes to the OS of cones exhibiting obvious disc morphogenesis defects due to DNKIF17 suggests that KIF17 is important for disc morphogenesis, but is not essential for high fidelity targeting of cone opsin. Although KIF17 may be essential in the process of disc assembly or for the delivery of cargo necessary for disc assembly, these findings suggest that the cargo may not be cone opsin. Instead, our results are consistent with previous data suggesting that kinesin II is necessary for proper trafficking of opsin into the OS (Marszalek et al., 2000;Lin-Jones et al., 2003;Jimeno et al., 2006). A potential inconsistency is our previous finding that cone opsin was mislocalized in cones of KIF17 morphants. This discrepancy may be related to the fact that OS formation was severely ablated in KIF17 morphants at a time when opsin synthesis persisted, while DNKIF17 resulted in a milder phenotype that involved disorganization of discs.

Our results with morpholino knockdown of KIF3B are consistent with a role for this motor in early embryonic development (Marszalek et al., 1999; Nonaka, et al., 1998). Kinesin II is a canonical IFT motor required for ciliogenesis and cilia have been shown to contribute to the transport of signals essential for early embryonic development (Caspary et al., 2007; Haycraft et al., 2007; Rohatgi et al., 2007; Corbit et al., 2008; Nielsen et al., 2008). Many of the early defects may have resulted from failed kinesin II dependent ciliogenesis or other cellular

NIH-PA Author Manuscript

NIH-PA Author Manuscript

NIH-PA Author Manuscript

functions of kinesin II. Although we cannot rigorously rule out toxic effects, the two KIF3B morpholinos, developed here are potentially useful tools for analysis of those early developmental defects.

Our use of targeted expression of DNKIF3B and DNKIF17 in 5 day old zebrafish cone photoreceptors allowed us to analyze the immediate effects of DN expression in cones that had already begun to develop their OS. This analysis was also facilitated by separate analysis of the early developing OS of the central retina with the less mature, late developing OS in the peripheral retina (Fig. 5). Surprisingly, cones expressing DNKIF3B started to die within 48 hours after fluorescence was initially detected at 3 dpf whereas cones expressing DNKIF17 exhibited little if any photoreceptor cell death. Many DNKIF3B-expressing photoreceptor IS that accumulated large vacuoles and dense material while retaining normal OS structure. This along with the strong mislocalization of cone opsin suggests that trafficking defects within the IS contribute to the photoreceptor degeneration seen with DNKIF3B. This interpretation is also supported by previous studies showing that depletion of kinesin II in mouse photoreceptors leads to ectopic accumulation of opsin and membranous material in the IS (Marszalek et al., 2000).

The inner segment defects described above could reflect a role for kinesin II in ER-Golgi trafficking as reported previously (Le Bot et al., 1998). Likewise, the lack of development of synaptic ribbons in cone pedicles could reflect an additional role for kinesin II in axonal transport and synaptic development. Although cone pedicles with invaginations from adjacent horizontal and bipolar cells were present in DNKIF3B-expressing embryos, synaptic ribbons were rarely seen. Impaired formation of ribbon synapses is consistent with prior work (Muresan, 2000) indicating a role for kinesin II in axonal transport, and raises the possibility that the kinesin II motor transports cargo to the pedicle. It has also been reported that KIF3A is a component of photoreceptor synaptic ribbons (Muresan et al., 1999). Since overexpressed DNKIF3B would be expected bind KIF3A to form non-functional complexes, DNKIF3B could also directly affect ribbon formation.

In a previous study in *Xenopus* (Lin-Jones et al., 2003), the rod opsin promoter was used to drive expression of DNKIF3B at a stage prior to rod OS formation. This resulted in a dramatic phenotype in which only a very restricted number of rods survived in tadpoles expressing the transgene. This prevented an extensive analysis of defects occurring prior to cell death. In contrast, our characterization of early ultrastructural defects was made possible by the use of the late onset cone transducin promoter (Kennedy et al., 2007). Although the late onset of transgene expression may explain our success in detecting early IS anomalies, we cannot rule out a somewhat different role for kinesin II in rods (Lin-Jones et al., 2003) compared to cones (this study).

Compared to DNKIF3B, late developing cones at the periphery expressing DNKIF17 had shorter OS (Fig. 4C). This suggests that KIF17 is required for OS elongation. Furthermore, in the central retina cones accumulate vesicles at the base of the OS but did not show IS defects. The failure to assemble discs at the base of the OS suggests that one or more components essential for disc assembly requires KIF17. Presumably, those components were still transported normally in DNKIF3B-expressing photoreceptors with early signs of degeneration. Reciprocally, the disruption of KIF17 trafficking did not seem to affect the targeting of cone opsin to the OS (Fig. 3).

Our data suggesting different roles for kinesin II and KIF17 in OS assembly may be related to earlier studies suggesting independent sorting pathways for rhodopsin and Peripherin-2/Rom-1, two OS membrane proteins essential for disc formation (Fariss et al., 1997; Lee et al., 2006). Further studies should determine whether peripherin-2 and ROM-1 are potential IFT

NIH-PA Author Manuscript

NIH-PA Author Manuscript

NIH-PA Author Manuscript

cargo transported by KIF17 because defective transport of these disc rim components could account for the proximal accumulation of OS vesicles observed in our study (Fig. 7C). Consistent with this idea, a plausible explanation for the difference in DNKIF17 and DNKIF3B phenotypes could be that kinesin II and KIF17 take different trafficking routes in the IS or are involved in transport of different cargo.

Experimental procedures

Antibodies

The anti-kinesin II antibodies include a monoclonal antibody K2.4 (Cole et al., 1993) obtained from Covance (Richmond, CA) and three monoclonal anti-KIF3A, anti-KIF3B and anti-KAP3a antibodies purchased from BD Biosciences (San Jose, CA). Polyclonal anti-KIF17 was obtained from Abcam (Cambridge, MA). Anti-cone opsin antibodies were gifts from Dr. T. S. Vihtelic at the University of Notre Dame (Vihtelic et al., 1999).

Immunocytochemistry

Immunocytochemistry was performed as described previously (Insinna et al., 2008) in 5 day old embryos expressing Ta-CP/GFP, Ta-CP/DNKIF3B and Ta-CP/DNKIF17 constructs. Double label confocal projections of GFP (green) and cone opsin (red) were acquired using a Leica TCS-SP2 confocal system.

Conventional electron microscopy

Zebrafish embryos (N=6 for each treatment group) fixed in 2% paraformaldehyde and 2% glutaraldehyde were prepared for conventional EM in the Medical College of Wisconsin core Electron Microscopy Facility as described previously (Pazour et al., 2002). For light microscopy, retinae (N=6 for each treatment) of morphants or transgene expressing embryos were cut in 1 μm sections rostrocaudally until the central retina was reached. Sections were stained with toluidine blue and examined under an epifluorescence microscope (Nikon, TE3000). Thin sections prepared from these blocks were stained with lead citrate and uranyl acetate and viewed using a Hitachi 600 or JEOL JEM 2100 electron microscope.

Immuno-electron microscopy

For immuno-EM we applied a recently introduced pre-embedding labeling technique (Maerker et al., 2008). Eyes of mature C57BL/6J mice were fixed in 4% buffered paraformaldehyde, infiltrated with 30% buffered sucrose and cracked by cycles of freezing in liquid nitrogen and thawing at 37°C. 50 μm thick vibratom sections were incubated with primary antibodies and biotinylated secondary antibodies (Vector Laboratories), and visualized by a Vectastain ABC-Kit (Vector Laboratories). After silver enhancement, post fixation and dehydration specimens were embedded in araldite. Ultrathin sections were analyzed in a Tecnai 12 BioTwin transmission electron microscope (FEI, Eindhoven, The Netherlands).

Immunoprecipitations and western blot

Retinae from C57Bl/6 adult mice or dark-adapted adult zebrafish were dissected, homogenized, and sonicated in IP lysis buffer (1% NP-40, 250 mM NaCl, 20mM Tris HCl pH6.8, 5% glycerol, 0.02% sodium azide) with a protease inhibitor cocktail (Roche, Mannheim, Germany). Extracts were centrifuged at 20,000 × *g* for 20 min at 4 °C. Antibodies were incubated on a rotator at 4 °C for 45 min with 50 microliters of protein G-Sepharose 4 Fast Flow (Amersham Biosciences) and phosphate buffered saline (PBS). Beads were washed with PBS, extract was added to each bead/antibody mixture and incubated for 2h at 4 °C. Beads were then washed three times in IP buffer and proteins were eluted from the beads by boiling in 2× Laemmli buffer. Western-blotting was performed as described previously (Insinna et al., 2008).

NIH-PA Author Manuscript

NIH-PA Author Manuscript

NIH-PA Author Manuscript

Morpholino design

The zebrafish *kif3b* mRNA was predicted in sequence (ZFIN database) based on protein homology to the mouse KIF3B (NP_032470) using tblastp. The translation-blocking, splice-blocking and control morpholino oligonucleotides used to knock-down zebrafish KIF3B were ordered from Gene Tools (Corvallis, OR, USA). Sequences of the KIF3B morpholinos were: aKIF3B: 5′- GTTGGCCTGCTGGATTCTCCGAATG -3′ spKIF3B: 5′-ATGGCCTGAGAGTAATGATAGGGTT -3′ control spKIF3B: 5′-AACCCTATCATTACTCTCTCAGGCCAT -3′. Morpholinos were injected using a nanoliter 2000 microinjector (World Precision Instruments, Inc) in 1-2 cell stage wild type TuAB embryos, at varying concentrations with an injection volume of 4.6nl/embryo. Injected embryos were kept in fish water containing 0.003% 1-phenyl-2-thiourea (PTU) to inhibit development of pigmentation. Western blotting was performed to verify the level of KIF3B protein knock-down.

DNKIF3B and DNKIF17 constructs

All clones were created by site-specific recombinational cloning using Invitrogen's MultiSite Gateway® Technology. A PCR fragment containing GFP and the *Xenopus* KIF3B stalk and tail (Le Bot et al., 1998; Lin-Jones et al., 2003) and site-specific attB recombination sites was used in the BP recombination reaction to create the DNKIF3B entry clone. A PCR fragment containing a mouse dominant negative KIF17 transgene with the motor domain replaced by GFP (Chu et al., 2006) and site-specific attB recombination sites was used in the BP recombination reaction to create the DNKIF17 entry clone. A PCR fragment containing the zebrafish cone transducin α promoter (Ta-CP) (Kennedy et al., 2007) and site-specific attB recombination sites was used in the BP recombination reaction to create the Ta-CP entry clone. The Ta-CP and DNKIF3B entry clones were used in the LR recombination reaction with pcDNA 6.2/V5-pL-DEST vector (Invitrogen, Carlsbad, CA) to create the Ta-CP-DNKIF3B expression clone used in the experiments. The Ta-CP and DNKIF17 entry clones were used in the LR recombination reaction with pcDNA 6.2/V5-pL-DEST vector to create the TaCP-DNKIF17 expression clones used in the experiments.

Acknowledgments

We thank Dr. Don Arnold for the DNKIF17 (USC, Los Angeles, CA), Dr. Beth Burnside (UC Berkeley, CA) for the DNKIF3B construct, and Dr. Breandan Kennedy (UCD, Ireland) for the Ta-CP promoter. We also thank Dr. Brian Link for access to the Medical College of Wisconsin zebrafish facility, and Clive Wells for assistance with EM imaging. This work was supported by NIH grant EY03222 (JCB), a NIH core grant for Vision Research, and Medical College of Wisconsin Research Development Funds (JCB). C. Insinna was supported by NIH NRSA Training grant T32-EY014537.

Grant sponsor: NIH grant EY03222, NIH NRSA Training grant T32-EY014537

References

Baker SA, Freeman K, Luby-Phelps K, Pazour GJ, Besharse JC. IFT20 links kinesin II with a mammalian intraflagellar transport complex that is conserved in motile flagella and sensory cilia. J Biol Chem 2003;278:34211–34218. [PubMed: 12821668]

Beech PL, Pagh-Roehl K, Noda Y, Hirokawa N, Burnside B, Rosenbaum JL. Localization of kinesin superfamily proteins to the connecting cilium of fish photoreceptors. J Cell Sci 1996;109(Pt 4):889–897. [PubMed: 8718680]

Branchek T, Bremiller R. The development of photoreceptors in the zebrafish, Brachydanio rerio. I. Structure. J Comp Neurol 1984;224:107–115. [PubMed: 6715574]

Caspary T, Larkins CE, Anderson KV. The graded response to Sonic Hedgehog depends on cilia architecture. Dev Cell 2007;12:767–778. [PubMed: 17488627]

NIH-PA Author Manuscript

NIH-PA Author Manuscript

NIH-PA Author Manuscript

Chu PJ, Rivera JF, Arnold DB. A role for Kif17 in transport of Kv4.2. J Biol Chem 2006;281:365–373. [PubMed: 16257958]

Cole DG, Chinn SW, Wedaman KP, Hall K, Vuong T, Scholey JM. Novel heterotrimeric kinesin-related protein purified from sea urchin eggs. Nature 1993;366:268–270. [PubMed: 8232586]

Cole DG, Diener DR, Himelblau AL, Beech PL, Fuster JC, Rosenbaum JL. Chlamydomonas kinesin-II-dependent intraflagellar transport (IFT): IFT particles contain proteins required for ciliary assembly in Caenorhabditis elegans sensory neurons. J Cell Biol 1998;141:993–1008. [PubMed: 9585417]

Corbit KC, Shyer AE, Dowdle WE, Gaulden J, Singla V, Chen MH, Chuang PT, Reiter JF. Kif3a constrains beta-catenin-dependent Wnt signalling through dual ciliary and non-ciliary mechanisms. Nat Cell Biol 2008;10:70–76. [PubMed: 18084282]

Deane JA, Cole DG, Seeley ES, Diener DR, Rosenbaum JL. Localization of intraflagellar transport protein IFT52 identifies basal body transitional fibers as the docking site for IFT particles. Curr Biol 2001;11:1586–1590. [PubMed: 11676918]

Evans JE, Snow JJ, Gunnarson AL, Ou G, Stahlberg H, McDonald KL, Scholey JM. Functional modulation of IFT kinesins extends the sensory repertoire of ciliated neurons in Caenorhabditis elegans. J Cell Biol 2006;172:663–669. [PubMed: 16492809]

Fariss RN, Molday RS, Fisher SK, Matsumoto B. Evidence from normal and degenerating photoreceptors that two outer segment integral membrane proteins have separate transport pathways. J Comp Neurol 1997;387:148–156. [PubMed: 9331178]

Haycraft CJ, Zhang Q, Song B, Jackson WS, Detloff PJ, Serra R, Yoder BK. Intraflagellar transport is essential for endochondral bone formation. Development 2007;134:307–316. [PubMed: 17166921]

Horst CJ, Johnson LV, Besharse JC. Transmembrane assemblage of the photoreceptor connecting cilium and motile cilium transition zone contain a common immunologic epitope. Cell Motil Cytoskeleton 1990;17:329–344. [PubMed: 1706225]

Insinna C, Pathak N, Perkins B, Drummond I, Besharse JC. The homodimeric kinesin, Kif17, is essential for vertebrate photoreceptor sensory outer segment development. Dev Biol 2008;316:160–170. [PubMed: 18304522]

Jimeno D, Feiner L, Lillo C, Teofilo K, Goldstein LS, Pierce EA, Williams DS. Analysis of kinesin-2 function in photoreceptor cells using synchronous Cre-loxP knockout of Kif3a with RHO-Cre. Invest Ophthalmol Vis Sci 2006;47:5039–5046. [PubMed: 17065525]

Kennedy BN, Alvarez Y, Brockerhoff SE, Stearns GW, Sapetto-Rebow B, Taylor MR, Hurley JB. Identification of a zebrafish cone photoreceptor-specific promoter and genetic rescue of achromatopsia in the nof mutant. Invest Ophthalmol Vis Sci 2007;48:522–529. [PubMed: 17251445]

Kljavin IJ. Early development of photoreceptors in the ventral retina of the zebrafish embryo. J Comp Neurol 1987;260:461–471. [PubMed: 3597842]

Kozminski KG, Beech PL, Rosenbaum JL. The Chlamydomonas kinesin-like protein FLA10 is involved in motility associated with the flagellar membrane. J Cell Biol 1995;131:1517–1527. [PubMed: 8522608]

Le Bot N, Antony C, White J, Karsenti E, Vernos I. Role of xklp3, a subunit of the Xenopus kinesin II heterotrimeric complex, in membrane transport between the endoplasmic reticulum and the Golgi apparatus. J Cell Biol 1998;143:1559–1573. [PubMed: 9852151]

Lee ES, Burnside B, Flannery JG. Characterization of peripherin/rds and rom-1 transport in rod photoreceptors of transgenic and knockout animals. Invest Ophthalmol Vis Sci 2006;47:2150–2160. [PubMed: 16639027]

Lin-Jones J, Parker E, Wu M, Knox BE, Burnside B. Disruption of kinesin II function using a dominant negative-acting transgene in Xenopus laevis rods results in photoreceptor degeneration. Invest Ophthalmol Vis Sci 2003;44:3614–3621. [PubMed: 12882815]

Maerker T, van Wijk E, Overlack N, Kersten FF, McGee J, Goldmann T, Sehn E, Roepman R, Walsh EJ, Kremer H, Wolfrum U. A novel Usher protein network at the periciliary reloading point between molecular transport machineries in vertebrate photoreceptor cells. Hum Mol Genet 2008;17:71–86. [PubMed: 17906286]

Marszalek JR, Liu X, Roberts EA, Chui D, Marth JD, Williams DS, Goldstein LS. Genetic evidence for selective transport of opsin and arrestin by kinesin-II in mammalian photoreceptors. Cell 2000;102:175–187. [PubMed: 10943838]

NIH-PA Author Manuscript

NIH-PA Author Manuscript

NIH-PA Author Manuscript

Marszalek JR, Ruiz-Lozano P, Roberts E, Chien KR, Goldstein LS. Situs inversus and embryonic ciliary morphogenesis defects in mouse mutants lacking the KIF3A subunit of kinesin-II. Proc Natl Acad Sci U S A 1999;96:5043–5048. [PubMed: 10220415]

Morris RL, Scholey JM. Heterotrimeric kinesin-II is required for the assembly of motile 9+2 ciliary axonemes on sea urchin embryos. J Cell Biol 1997;138:1009–1022. [PubMed: 9281580]

Mukhopadhyay S, Lu Y, Qin H, Lanjuin A, Shaham S, Sengupta P. Distinct IFT mechanisms contribute to the generation of ciliary structural diversity in C. elegans. EMBO J 2007;26:2966–2980. [PubMed: 17510633]

Muresan V. One axon, many kinesins: What's the logic? J Neurocytol 2000;29:799–818. [PubMed: 11466472]

Muresan V, Bendala-Tufanisco E, Hollander BA, Besharse JC. Evidence for kinesin-related proteins associated with the axoneme of retinal photoreceptors. Exp Eye Res 1997;64:895–903. [PubMed: 9301470]

Muresan V, Lyass A, Schnapp BJ. The kinesin motor KIF3A is a component of the presynaptic ribbon in vertebrate photoreceptors. J Neurosci 1999;19:1027–1037. [PubMed: 9920666]

Nielsen SK, Mollgard K, Clement CA, Veland IR, Awan A, Yoder BK, Novak I, Christensen ST. Characterization of primary cilia and Hedgehog signaling during development of the human pancreas and in human pancreatic duct cancer cell lines. Dev Dyn 2008;237:2039–2052. [PubMed: 18629868]

Nonaka S, Tanaka Y, Okada Y, Takeda S, Harada A, Kanai Y, Kido M, Hirokawa N. Randomization of left-right asymmetry due to loss of nodal cilia generating leftward flow of extraembryonic fluid in mice lacking KIF3B motor protein. Cell 1998;95:829–837. [PubMed: 9865700]

Pan X, Ou G, Civelekoglu-Scholey G, Blacque OE, Endres NF, Tao L, Mogilner A, Leroux MR, Vale RD, Scholey JM. Mechanism of transport of IFT particles in C. elegans cilia by the concerted action of kinesin-II and OSM-3 motors. J Cell Biol 2006;174:1035–1045. [PubMed: 17000880]

Pazour GJ, Baker SA, Deane JA, Cole DG, Dickert BL, Rosenbaum JL, Witman GB, Besharse JC. The intraflagellar transport protein, IFT88, is essential for vertebrate photoreceptor assembly and maintenance. J Cell Biol 2002;157:103–113. [PubMed: 11916979]

Qin H, Diener DR, Geimer S, Cole DG, Rosenbaum JL. Intraflagellar transport (IFT) cargo: IFT transports flagellar precursors to the tip and turnover products to the cell body. J Cell Biol 2004;164:255–266. [PubMed: 14718520]

Rohatgi R, Milenkovic L, Scott MP. Patched1 regulates hedgehog signaling at the primary cilium. Science 2007;317:372–376. [PubMed: 17641202]

Scholey JM. Intraflagellar transport motors in cilia: moving along the cell's antenna. J Cell Biol. 2008

Snow JJ, Ou G, Gunnarson AL, Walker MR, Zhou HM, Brust-Mascher I, Scholey JM. Two anterograde intraflagellar transport motors cooperate to build sensory cilia on C. elegans neurons. Nat Cell Biol 2004;6:1109–1113. [PubMed: 15489852]

Tam BM, Moritz OL, Hurd LB, Papermaster DS. Identification of an outer segment targeting signal in the COOH terminus of rhodopsin using transgenic Xenopus laevis. J Cell Biol 2000;151:1369–1380. [PubMed: 11134067]

Vihtelic TS, Doro CJ, Hyde DR. Cloning and characterization of six zebrafish photoreceptor opsin cDNAs and immunolocalization of their corresponding proteins. Visual Neurosci 1999;16:571–585.

Whitehead JL, Wang SY, Bost-Usinger L, Hoang E, Frazer KA, Burnside B. Photoreceptor localization of the KIF3A and KIF3B subunits of the heterotrimeric microtubule motor kinesin II in vertebrate retina. Exp Eye Res 1999;69:491–503. [PubMed: 10548469]

NIH-PA Author Manuscript
NIH-PA Author Manuscript
NIH-PA Author Manuscript

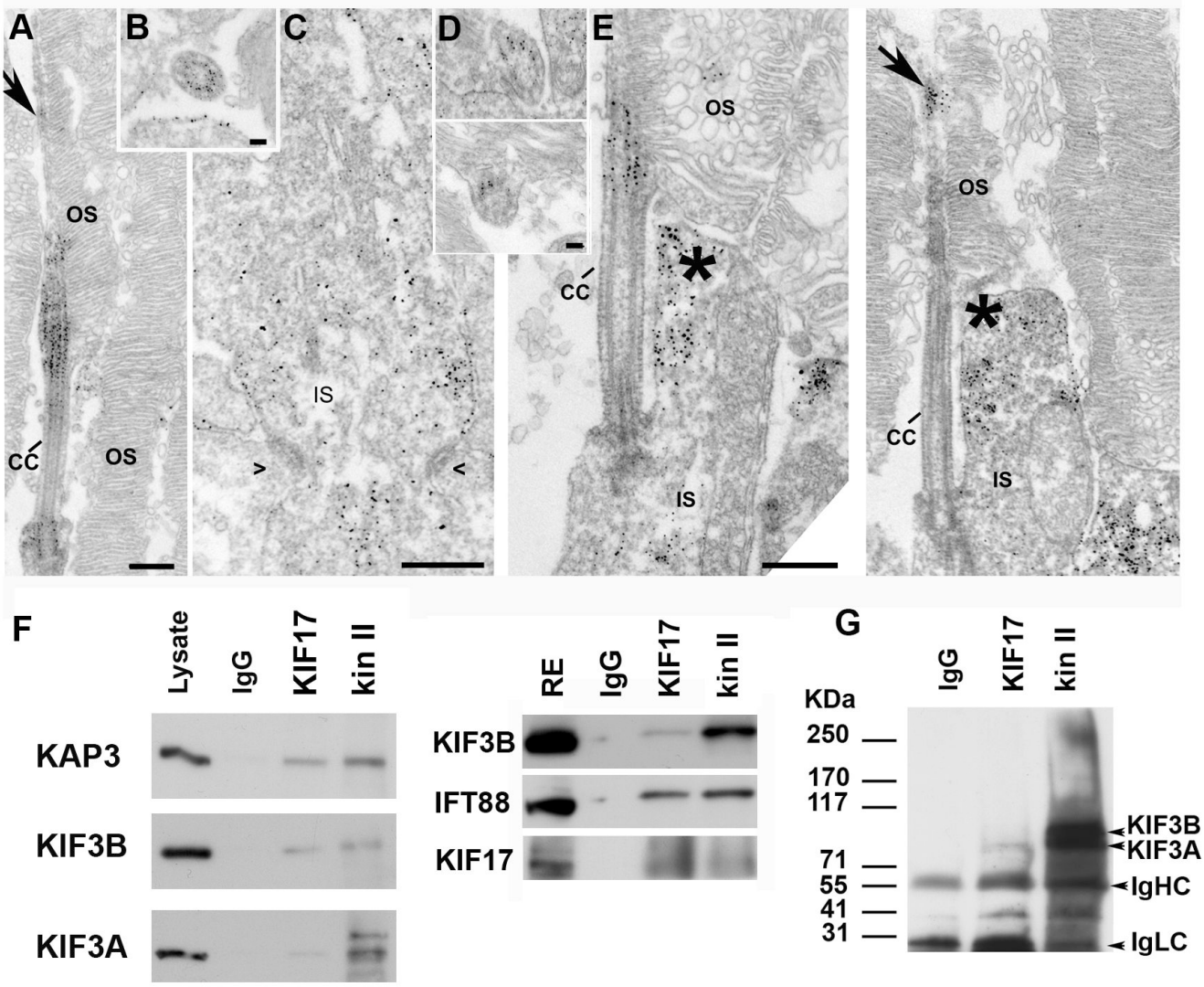

Fig. 1. KIF17 and kinesin II localization and co-immunoprecipitation

A-C. Immuno-EM localization of the KAP3 subunit of kinesin II in mouse rod photoreceptor cells. **A.** Longitudinal section through the connecting cilium and parts of the outer segment (OS). Bar = 400 nm. **B.** Cross section through the CC. Bar = 50 nm. **C.** Section through in the ER-Golgi region of the IS. Bars = 400 nm. Symbols (><) indicate position of adherens junctions at the outer limiting membrane. **D-E.** Immuno-EM localization of KIF17. **D.** Two slightly oblique sections through the CC. Bar = 50 nm in upper panel and 100 nm in lower panel. **E.** Two longitudinal images through the photoreceptor at the level of the CC. Arrow points to labeling in the axoneme of the OS. Asterisks indicate labeling in the collar-like extension of the apical IS. Bars = 400 nm. **F.** Co-immunoprecipitation from mouse retinal extracts of either kinesin II or KIF17 with IFT88. IP antibodies are shown at the top. Western blots were done with antibodies for KIF17, IFT88, and the three kinesin II subunits (KAP3, KIF3B and KIF3A); antibodies and are shown on the left. A mixture of IgGs was used as control for non-specific binding. **G.** IP experiment as in **F** from zebrafish retinal extract; the kinesin II antibody (K2.4) recognizes both KIF3A and KIF3B.

NIH-PA Author Manuscript
NIH-PA Author Manuscript
NIH-PA Author Manuscript

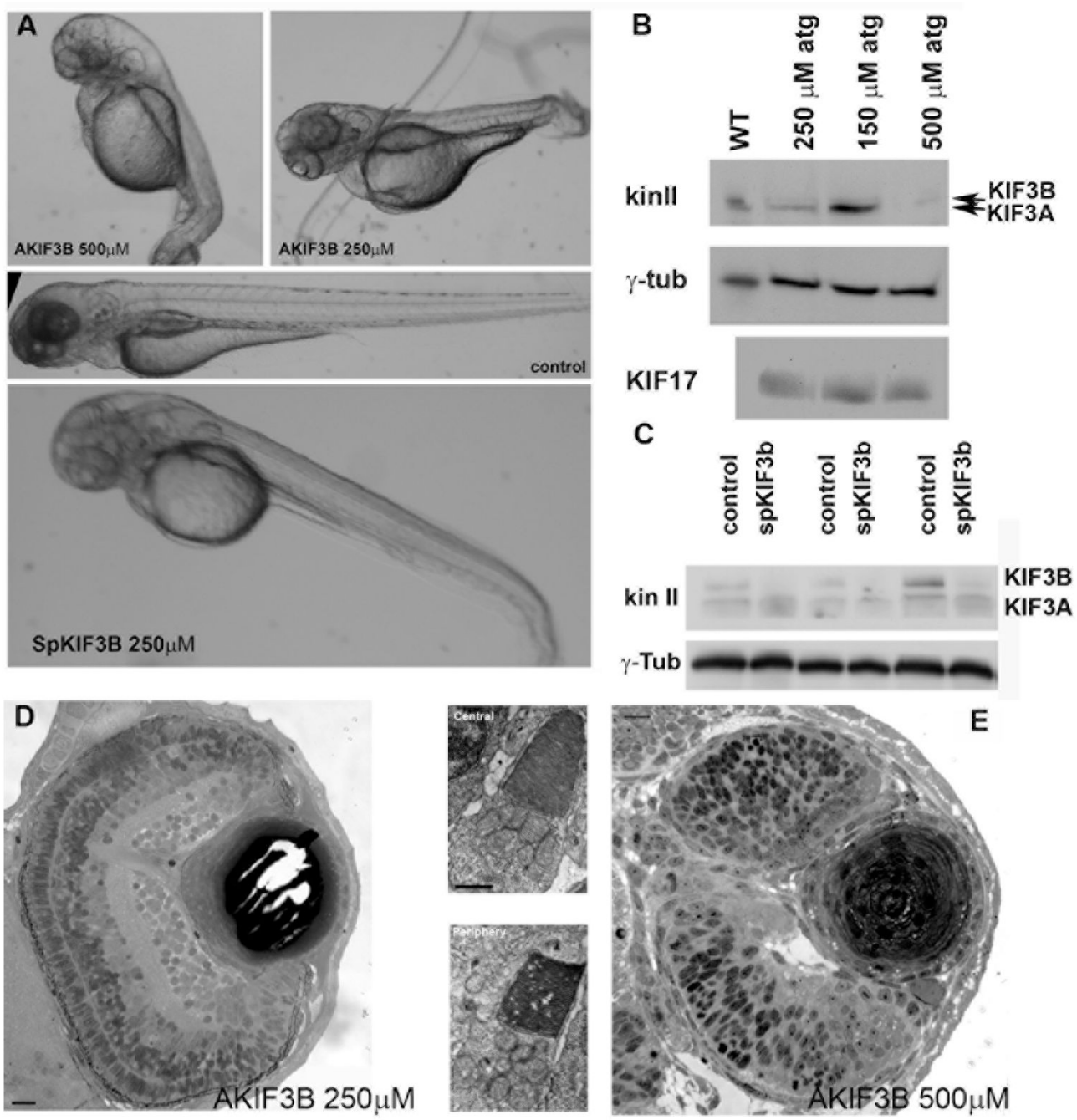

Fig. 2. Disruption of *kif3B* expression by an antisense morpholino oligonucleotide

A (upper panel). Images of three day old larvae that survived an injection of 500 μM (AKIF3B 500 μM) or 250 μM (AKIF3B 250 μM) of the translation-blocking morpholino. **A** (middle panel). A control injected embryo. **A** (lower panel). Three day old larva after injection with 250 μM of a splice-blocking morpholino (SpKIF3B). **B.** Western blots of whole embryo extracts showing the reduction of KIF3B and KIF3A in AKIF3B morphants at 3 dpf; anti-KIF17 and anti-γ-tubulin were used as controls. **C.** Western blot of three separate whole SpKif3B (250 μM) morphant and control embryo extracts showing similar depletion of KIF3B and KIF3A as observed in translation-blocking morphants (**B** above); anti- γ- tubulin was used as a loading control. **D.** Semi-thin section of the eye of an AKIF3B (250 μM) morphant at 3

dpf. Bar = 10 μm. Insets: EM views of AKIF3B (250 μM) photoreceptors. Bar = 2.5 μm. **E.** Semi-thin section of the eye of an AKIF3B (500 μM) morphant at 3 dpf. Note the absence of retinal lamination and photoreceptor differentiation. Bar = 10 μm.

NIH-PA Author Manuscript
NIH-PA Author Manuscript
NIH-PA Author Manuscript

NIH-PA Author Manuscript
NIH-PA Author Manuscript
NIH-PA Author Manuscript

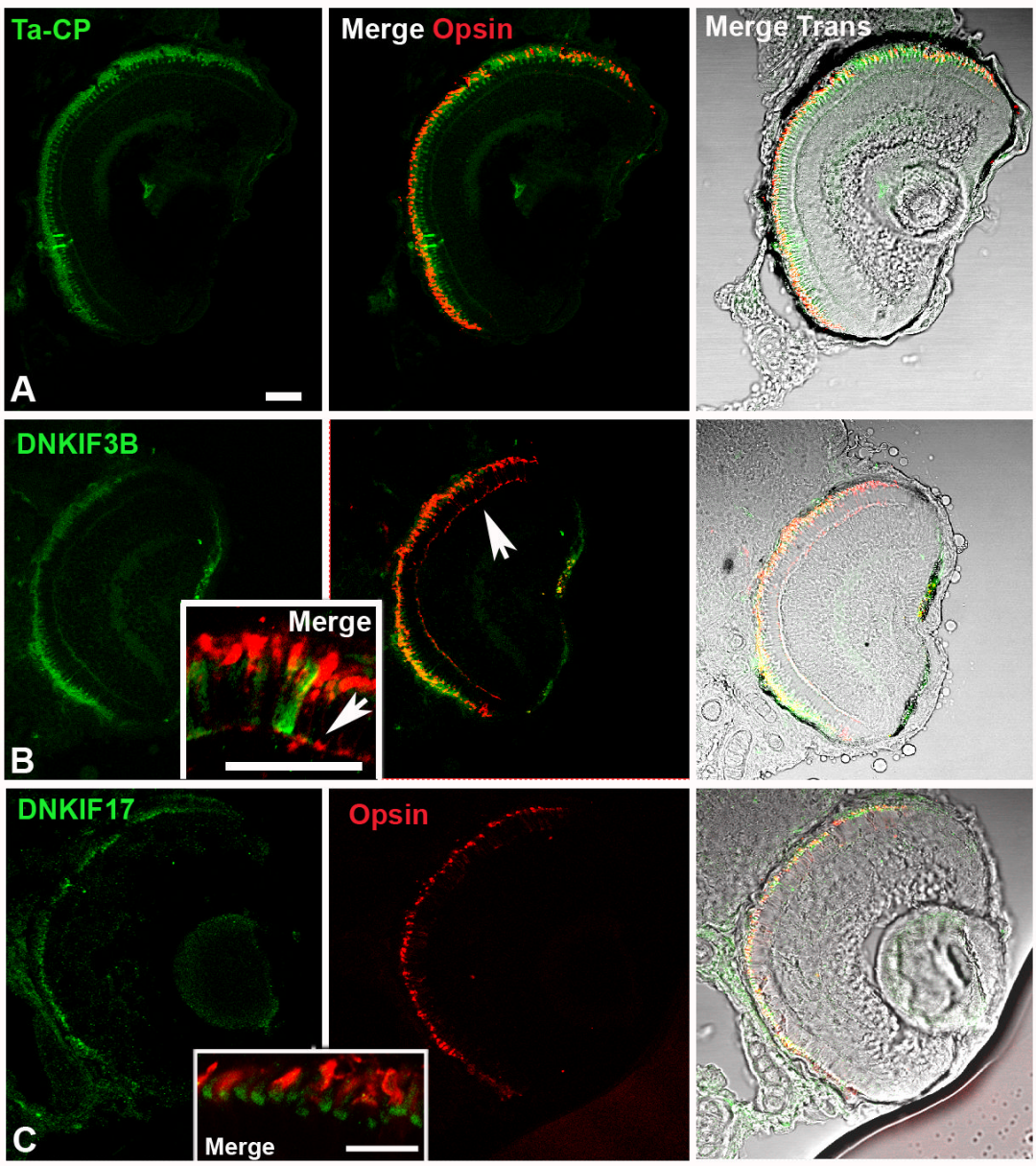

Fig. 3. Localization of Ta-CP directed expression of GFP, DNKIF3B and DNKIF17 and cone opsin localization at 5 dpf

The Ta-CP promoter up stream of GFP, DNKIF3B or DNKIF17 was injected at the 1 cell stage. **A.** In Ta-CP/GFP embryos GFP fluorescence was seen throughout the outer retina and cone opsin was highly localized to the OS. Bar = 10 μm and applies to panels **A-C. B.** In Ta-CP/DNKIF3B embryos transgene expression (GFP, green) was similar to controls, but cone opsin was mislocalized to the perinuclear region and outer plexiform layer (arrow) across the entire retina. Inset: Higher power image showing cone opsin mislocalization to the synaptic layer (arrow). Bar = 10 μm. **C.** In Ta-CP/DNKIF17 embryos transgene expression (GFP, green) was distributed across the entire retina, but was largely restricted to the IS (see inset). Cone opsin was in the OS and there was no evidence of mislocalization. Inset: Higher power image showing lack of mislocalization of cone opsin and strong accumulation of DNKIF17 in the IS. Bar = 10 μm.

NIH-PA Author Manuscript
NIH-PA Author Manuscript
NIH-PA Author Manuscript

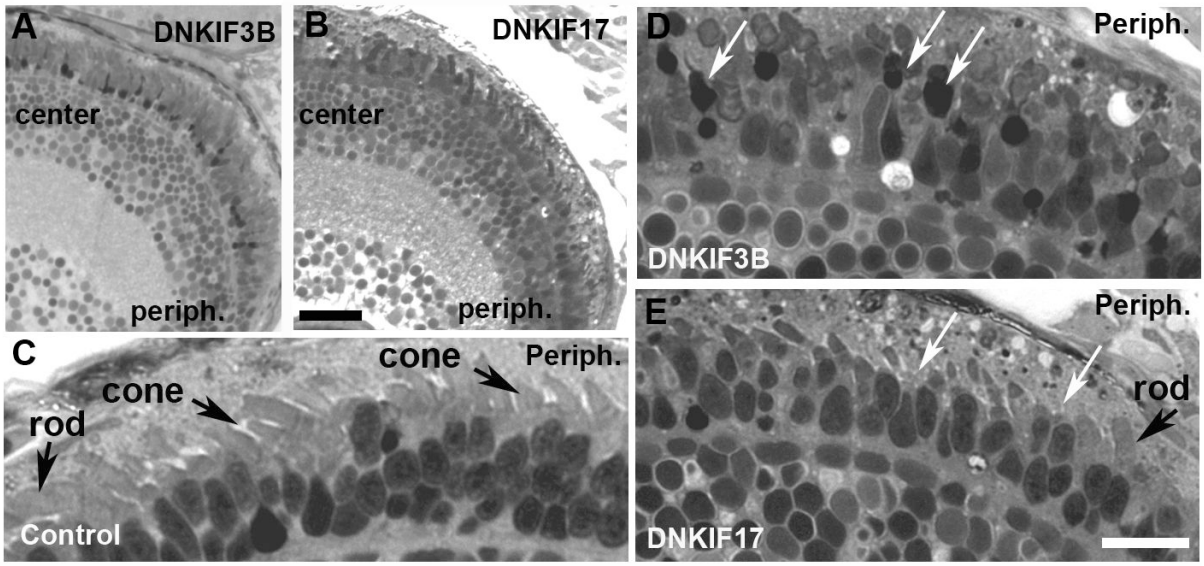

Fig. 4. Light microscopy of retinae of control, DNKIF3B and DNKIF17 embryos at 5 dpf

A-B. Low power images of semi-thin plastic sections of DNKIF3B (**A**) and DNKIF17 (**B**) eyes. Central (center) and peripheral (periph) retinal regions are labeled. Bar in B = 10 μm. **C.** Higher power image of the outer retina of a control eye; the periphery is on the right (Periph). Cone and rod OS are indicated by arrows. **D-E.** Higher power images of outer retina of DNKIF3B (**D**) and DNKIF17 (**E**) eyes; the periphery is on the right (periph). White arrows in **D** indicate condensed nuclei and cell bodies of dying cones. White arrows in **E** indicate cones with very short or missing OS. A normal rod OS is indicated in **E**, The bar in **E** = 10 μm and applies to **C-E**).

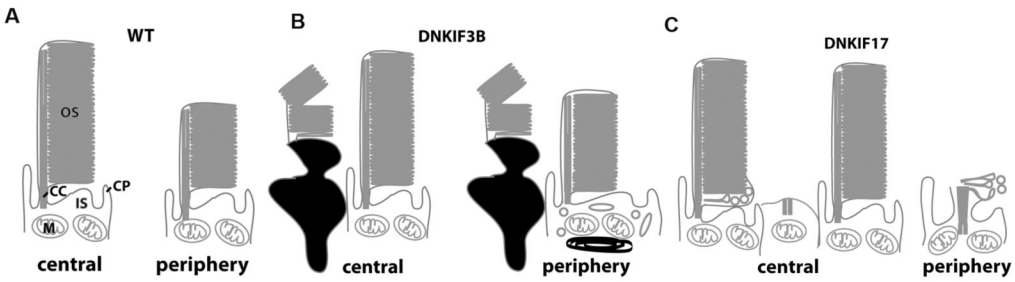

Fig. 5. Summary of the structural phenotypes observed in DNKIF3B and DNKIF17 embryos

A. In wild type retinae, cones of the central retina are more developed with longer OS than those at the periphery. CC, connecting cilium. CP, calycal process. **B.** In embryos expressing DNKIF3B many cells in the central and peripheral retina exhibit a condensed morphology suggesting an apoptotic state. In the periphery many uncondensed cones also exhibit IS vesicles and accumulation of dense material while retaining normal OS structure. **C.** In embryos expressing DNKIF17 cones in the central retina with normal IS exhibit accumulations of vesicles in the proximal OS opposite the cilium, but this phenotype is not seen in all cells. In the periphery, OS do not elongate and are often vesiculated. Cones do not exhibit features associated with excess apoptosis.

NIH-PA Author Manuscript
NIH-PA Author Manuscript
NIH-PA Author Manuscript

NIH-PA Author Manuscript
NIH-PA Author Manuscript
NIH-PA Author Manuscript

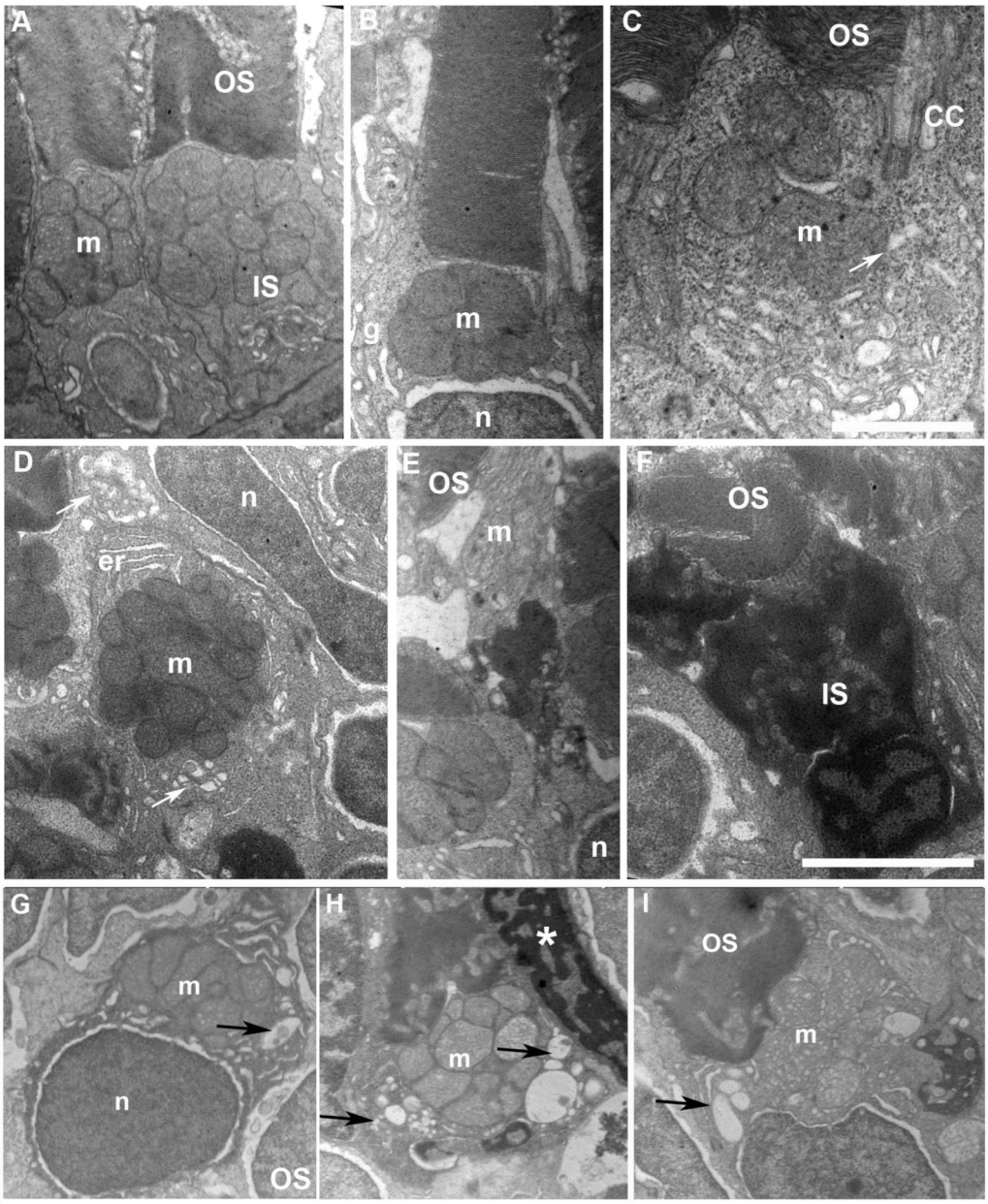

Fig. 6. Accumulation of large vacuoles and dense material in the IS of cones expressing DNKIF3B

A. EM view of cones at 5 days after injection of the Ta-CP driving GFP alone (control). Note the normal structure of OS discs and IS with accumulation of mitochondria (m) in the ellipsoid region. **B and C.** EM view of cones at 5 days after injection of the Ta-CP driving DNKIF3B showing mild IS defects. This was primarily enlargement of the cytoplasmic area around the mitochondria. Arrow indicates large vesicle below the CC. n, photoreceptor nucleus. g, golgi apparatus. Bar in C = 1.5 μm. **D.** EM view of a cross-section through the IS of a cone with a mild IS phenotype involving enlargement of the cytoplasmic area around mitochondria; er, endoplasmic reticulum. The upper arrow indicates accumulation of large vesicles in the ellipsoid region. The lower arrow indicates a Golgi region. **E.** EM view of a cone in the central retina that has a highly condensed IS between the nucleus (n) and mitochondrial rich (m) ellipsoid region. OS discs are normal. **F.** Cone with a highly condensed nucleus and IS with normal OS organization. Bar = 2.5 μm. **G-H.** Examples of cones accumulating vesicles and

large vacuoles (arrows) within the IS surrounding the mitochondria. Asterisk in H indicates condensed nucleus of an adjacent cone.

NIH-PA Author Manuscript
NIH-PA Author Manuscript
NIH-PA Author Manuscript

NIH-PA Author Manuscript
NIH-PA Author Manuscript
NIH-PA Author Manuscript

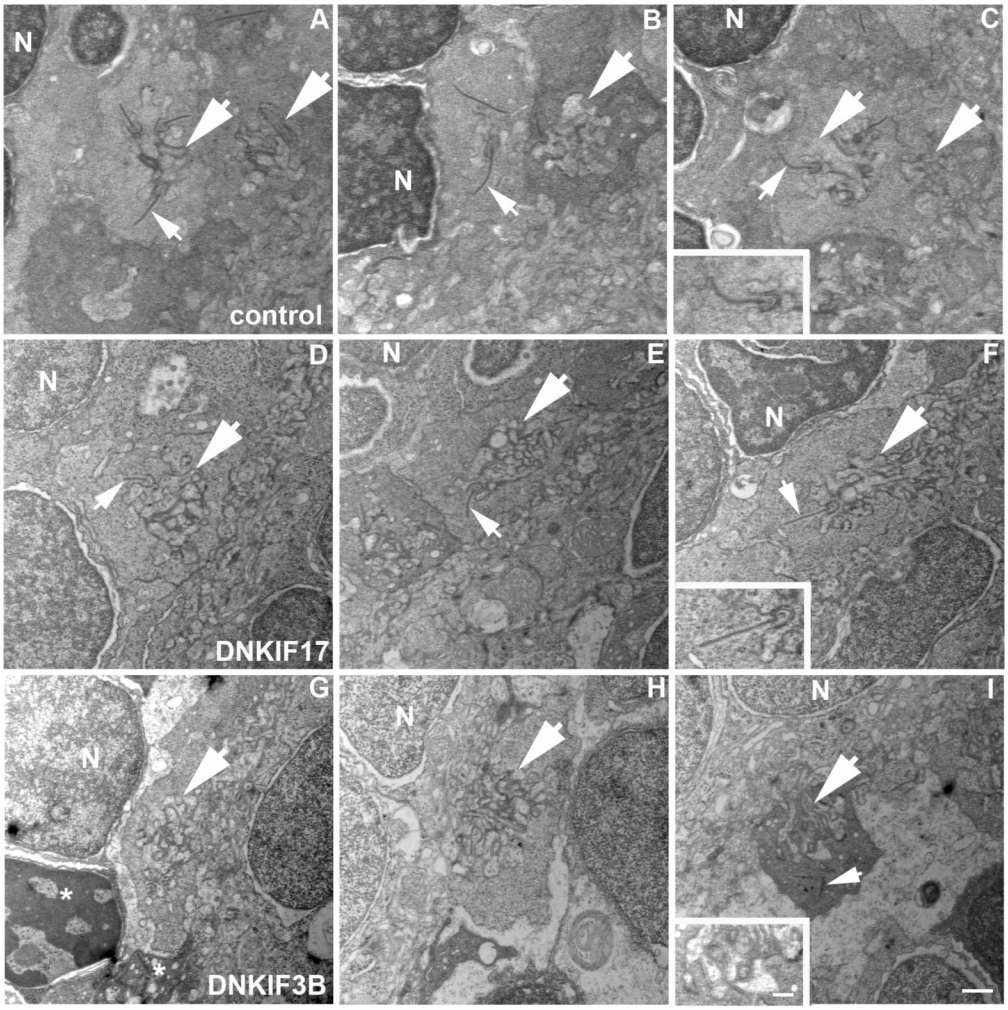

Fig. 7. Lack of synaptic ribbons in cone pedicles of DNKIF3B expressing embryos

A-C. Control pedicles showing post-synaptic invaginations (large arrows) and synaptic ribbons (small arrows) associated with pre-synaptic membranes. **D-F.** DNKIF17 cone pedicles showing post-synaptic invaginations (large arrows) and synaptic ribbons (small arrows) associated with pre-synaptic membranes. **G-I.** DNKIF3B cone pedicles showing post-synaptic invaginations (large arrows) without synaptic ribbons. Occasionally, ribbons are seen dissociated from presynaptic membranes (small arrow in **I**). Condensed nuclei and pedicles (asterisks) of dying cells are seen in G. Insets in **C**, **F**, and **I** are enlargements of invaginations to show association of ribbons with the presynaptic membrane. Bars in **I** and in inset = 500 nm.

NIH-PA Author Manuscript
NIH-PA Author Manuscript
NIH-PA Author Manuscript

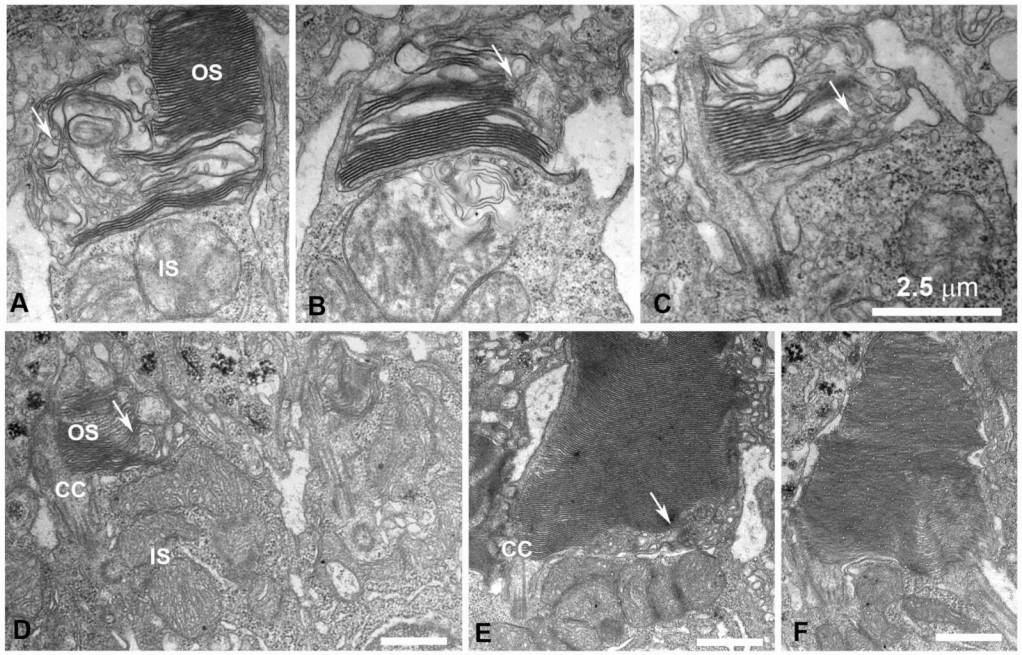

Fig. 8. Disruption of the OS structure in cones expressing DNKIF17

A-D. EM views of cones at the retinal periphery at 5 days after injection of Ta-CP driving DNKIF17. Note disrupted OS structure with failure to complete disc edges as shown by arrows. **E.** EM view of a cone in the central retina accumulating vesicular membranes within the base of the OS (arrows) opposite the cilium (CC). **F.** Normal rod photoreceptor. All bars = 2.5 μm; the bar in **C** applies to **A-C**.